Fission of odd-A and doubly odd actinide nuclei induced by direct reactions*

B. B. Back,† H. C. Britt, Ole Hansen,† and B. Leroux‡
Los Alamos Scientific Laboratory, University of California, Los Alamos, New Mexico 87544

J. D. Garrett§
Los Alamos Scientific Laboratory, University of California, Los Alamos, New Mexico 87544 and Brookhaven National Laboratory, Upton, New York 11973

(Received 23 May 1974)

Fission probability distributions have been measured using (d,pf), (t,pf), $(^3\mathrm{He},df)$, $(^3\mathrm{He},\alpha f)$, and $(t,\alpha f)$ reactions to excite a variety of odd-A and odd-odd actinide nuclei. Fission of the residual nuclei ^{229,231}Th, ^{231,232,233}Pa, ^{234,235,236,237,238,239}Np, ^{241}Pu, ^{240,241,243,245,247}Am, ^{249}Cm, and ^{249}Bk was studied. These results and other data available from previous (d,pf), (t,pf), and (n,f) studies are analyzed with a statistical model to obtain estimates of the heights and curvatures of one or both peaks of the double humped fission barrier. Estimates of barrier parameters are obtained for the above nuclei and for ^{233}Th, ^{235,237,239}U, ^{239,243,245}Pu, ^{242,244}Am, ^{245,247}Cm, and ^{253}Cf. Systematic variations of the barrier parameters are discussed.

[NUCLEAR REACTIONS, FISSION Measured fission probabilities, $E^* \leq 7.5$ MeV for ^{229,231}Th, ^{231,232,233}Pa, ^{234,235,236,237,238,239}Np, ^{241}Pu, ^{240,241,243,245,247}Am, ^{249}Cm, and ^{249}Bk using (d,pf), (t,pf), $(^3\mathrm{He},df)$, $(^3\mathrm{He},\alpha f)$, and $(t,\alpha f)$ reactions. Deduced properties of the double peaked fission barrier for these nuclei and for ^{233}Th, ^{235,237,239}U, ^{239,243,245}Pu, ^{242,244}Am, ^{245,247}Cm, and ^{253}Cf.]

I. INTRODUCTION

In a previous paper[1] results were presented on the fission of doubly even nuclei excited by a variety of direct reactions. In many cases subbarrier resonance structures were observed in the fission probabilities and these resonances were interpreted as vibrational excitations in the second potential well. A detailed statistical model of the direct-reaction induced fission process which included resonant penetration of the double humped fission barrier was used to analyze the experimental results and estimates of the heights and curvatures of the two barrier peaks were extracted. The observed resonance structures were significantly broader than predicted from the penetrabilities of the two peaks of the barrier because of damping in the second well,[1-3] resulting from the coupling between the vibrational excitations and other compound excitations.

These same direct reaction techniques can be used to study odd-A and doubly odd nuclei. For these cases it is generally found that the fission probability distributions do not show subbarrier resonances. The lack of observable resonance structures in odd-A and doubly odd nuclei has been attributed[3] in part to an increased damping caused by the higher density of compound states in the second well as compared to even-even cases and in part to an increased density of fission transition states. These experimental fission probabilities which do not show resonant structures can be reproduced by a statistical model in which a complete damping of the vibrational strength in both wells is assumed. In this limit the penetrabilities through the two peaks of the barrier are treated incoherently. These calculations require an estimate of the spectrum of fission transition states which is more complex for odd nuclei than for the doubly even nuclei and it is also necessary to consider competition with neutron decay as well as γ emission. These requirements lead to a statistical model for describing the direct-reaction induced fission of odd nuclei different from the one used for treating the even-even nuclei.

In this paper we present experimental data on fission probability distributions for a number of odd-A and doubly odd isotopes of Th, Pa, Np, Pu, Cm, and Bk. A statistical model for the direct-reaction induced fission process is developed and used to analyze the present data as well as previous results from (n,f), (d,pf), and (t,pf) studies. The analysis yields estimates of the height and curvature of the highest peak of the fission barrier or, in some cases, of the heights of both peaks of the barrier. These barrier heights, combined with results from the analysis of fission probabilities for even-even nuclei and with results from analysis of fission isomer excitation functions, yield a detailed picture of the systematic behavior of fission barriers in the actinide region.

II. EXPERIMENTAL RESULTS

A. Experimental setup

The experimental setup was identical to that described in detail in the previous paper.[1] Therefore, only a brief outline of the most important features will be given here.

The setup is illustrated schematically in Fig. 1. The outgoing reaction particle is identified and its energy measured with a resolution of 60–150 keV in a standard ΔE-E counter telescope placed at an angle near 90°. For each event the excitation energy of the residual nucleus is determined from the kinetic energy of the outgoing reaction particle. In the experiment the spectrum of reaction particles is measured both in a configuration where a coincidence is required with a large annular fission detector (coincidence spectrum) and in a configuration where no coincidence is required (singles spectrum). Using a measured solid angle for the fission detector and assuming that the coincident fission fragments are isotropically distributed, the ratio of coincidence to singles spectra can be transformed to a distribution of fission probability as a function of excitation energy in the fissioning nucleus. Due to the large solid angle of the fission detector, the assumption that the fragments have an isotropic angular correlation is found to be adequate for the determination of the fission probability distributions.[1]

The absolute energy scales are determined from a calibration of the counter telescope with known energy lines from appropriate reactions on lead targets. Absolute excitation energies determined in this manner are believed to be accurate to ±50 keV. Systematic errors in the absolute fission probabilities are believed to be less than ±20% for (^{3}He, df) cases, ±30% for (t, pf) cases, and ±40% for (t, αf) and (^{3}He, αf) cases. For (d, pf) reactions to excitation energies above the neutron binding energy systematic uncertainties in the fission probabilities are estimated to be less than ±30% with part of this estimate being due to uncertainties in the corrections for protons coming from deuteron breakup reactions. Corrections applied to the (d, pf) results to account for this breakup are described in more detail in a later section.

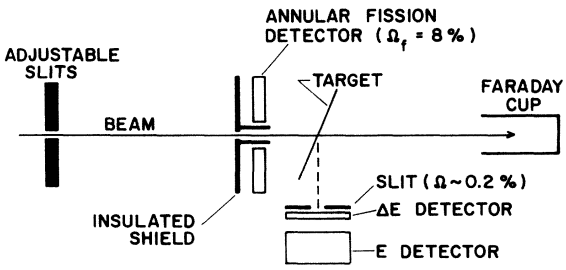

FIG. 1. Schematic diagram of the experimental setup.

B. Experimental data

The odd-A and doubly odd nuclei which were studied in this experiment are listed in Table I along with various experimental conditions for each measurement. Also listed in Table I are the results from previous (d, pf), (t, pf), and (n, f) studies[3–9] that we will analyze with the statistical model described in a later section. The energy scale for the (t, pf) results from Ref. 6 has been shifted by 0.1 MeV to allow for the systematic deviations of these results from the present measurements (see Ref. 1 for discussion).

The results obtained in the present experiment are shown in Figs. 2–5. The singles spectra have been normalized to indicate the magnitude of the accidental correction which was applied to the coincidence measurements. For (d, pf) and (t, pf) reactions, strong peaks are observed in the singles spectra from reactions on carbon and oxygen impurities in the target. In calculating fission probabilities the extrapolations indicated as solid lines in Figs. 2–5 were used as estimates of the singles rate from the actinide element.

In previous analyses of direct-reaction induced fission data[1,3,6] it has been assumed that the fission decay does not depend on the type of reaction used to excite the nucleus except for effects due to the different parity and total angular momentum distributions for the fissioning nuclei. This assumption has been tested[6] by comparing (n, f) and (t, pf) reactions involving the same fissioning nuclei and finding that the fission probability distributions are essentially the same. In Fig. 6 we compare experimental fission probabilities from the present experiment for ^{239}Np excited by both (^{3}He, df) and (t, pf) reactions and it is seen that the results agree within the estimated error on the absolute fission probabilities (±20%). In Fig. 6 we also compare our results for the ^{237}Np(d, pf) reaction with the previous measurement of Back *et al.*[3] and it is seen that they agree reasonably well.

III. (n, f) AND (d, pf) DATA FROM PREVIOUS MEASUREMENT

The (n, f) and (d, pf) reactions lead to the same fissioning nuclei but it is not possible to directly compare the experimental results. In the case of odd neutron nuclei neither reaction gives a direct measurement of the fission probability. For (n, f)

TABLE I. Various experimental conditions for odd-A and doubly odd nuclei studied, and results from previous studies.

Compound nucleus	Reaction	Target	Beam energy (MeV)	Detector angle	Detector resolution (keV)	P_f^{max}	Reference
^{229}Th	^{3}He,α	^{230}Th	24	90°	135	0.11	Present exp.
^{231}Th	d,p	^{230}Th	15	90°	75	0.10	Present exp.
^{233}Th	n,f	^{232}Th	...	...	...	0.035	Ref. 4.
^{231}Pa	^{3}He,d	^{230}Th	24	90°	80	0.50	Present exp.
^{232}Pa	d,p	^{231}Pa	15	100°	55	0.22	Present exp.
^{233}Pa	^{3}He,d	^{232}Th	24	90°	80	0.68	Present exp.
^{235}U	t,p	^{233}U	18	130°	~120	0.40	Ref. 6.
^{237}U	t,p	^{235}U	18	150°	~120	0.28	Ref. 6.
^{239}U	n,f	^{238}U	...	...	...	0.18	Ref. 5.
^{234}Np	^{3}He,d	^{233}U	24	90°	95	0.79	Present exp.
^{235}Np	^{3}He,d	^{234}U	24	90°	110	0.69	Present exp.
^{236}Np	^{3}He,d	^{235}U	24	90°	80	0.64	Present exp.
^{237}Np	^{3}He,d	^{236}U	24	90°	100	0.66	Present exp.
^{238}Np	d,p	^{237}Np	15	90°	50	0.55	Present exp.
^{239}Np	^{3}He,d	^{238}U	24	90°	105	0.72	Present exp.
^{239}Pu	d,p	^{238}Pu	13	140°	...	0.48	Ref. 3.
^{241}Pu	t,p	^{239}Pu	15	90°	85	0.33	Present exp.
^{243}Pu	n,f	^{242}Pu	...	...	...	0.49	Ref. 7.
^{245}Pu	n,f	^{244}Pu	...	...	...	0.30	Ref. 7.
^{240}Am	^{3}He,d	^{239}Pu	24	90°	125	0.63	Present exp.
^{241}Am	^{3}He,d	^{240}Pu	24	90°	125	0.34	Present exp.
^{242}Am	d,p	^{241}Am	13	140°	...	0.54	Ref. 3.
^{243}Am	^{3}He,d	^{242}Pu	24	90°	125	0.65	Present exp.
^{244}Am	d,p	^{243}Am	13	140°	...	0.44	Ref. 3.
^{245}Am	t,p	^{243}Am	15	90°	65	0.54	Present exp.
^{247}Am	t,α	^{248}Cm	16	90°	145	0.83	Present exp.
^{245}Cm	n,f	^{244}Cm	...	...	...	0.60	Ref. 8.
^{247}Cm	n,f	^{246}Cm	...	...	...	0.50	Ref. 8.
^{249}Cm	d,p	^{248}Cm	15	90°	75	0.48	Present exp.
^{249}Bk	^{3}He,d	^{248}Cm	24	90°	70	0.51	Present exp.
^{253}Cf	n,f	^{252}Cf	...	...	...	...	Ref. 9.

reactions the fission probability is obtained by dividing the measured fission cross section by a calculated total capture cross section, and for (d,pf) reactions at excitation energies above the neutron binding energy a significant correction must be made for contributions to the proton spectrum from deuteron breakup reactions. In a previous paper[6] calculations of fission probabilities from (n,f) cross section data are described. In addition, an empirical correction for deuteron breakup effects in (d,pf) reactions was developed from comparisons of (t,pf), (d,pf), and (n,f) results. The correction function determined by Britt and Cramer[6] has been applied to the (d,pf) data obtained in the present experiment and to the results of Back *et al.*[3] for the nuclei listed in Table I. A comparison of the corrected fission probabilities from (d,pf) reactions with fission probabilities obtained from (n,f) results[10] using the total reaction cross sections described previously[6] is shown in Fig. 7 for six different cases from ^{232}Pa through ^{249}Cm. It is seen that, except for ^{239}Pu, the agreement between (d,pf) and (n,f) results is very good. This agreement is even more remarkable since the (d,pf) experiments were performed under different conditions (deuteron energy and proton angle) than those in Ref. 6 where the breakup correction was determined. There is no *a priori* reason to expect this breakup correction to be independent of the experimental conditions but at least in these cases the previous correction function seems to work satisfactorily. The reason for the disagreement in ^{239}Pu is not clear but may be due to a normalization error in one of the experiments, both of which involve the very difficult target ^{238}Pu.

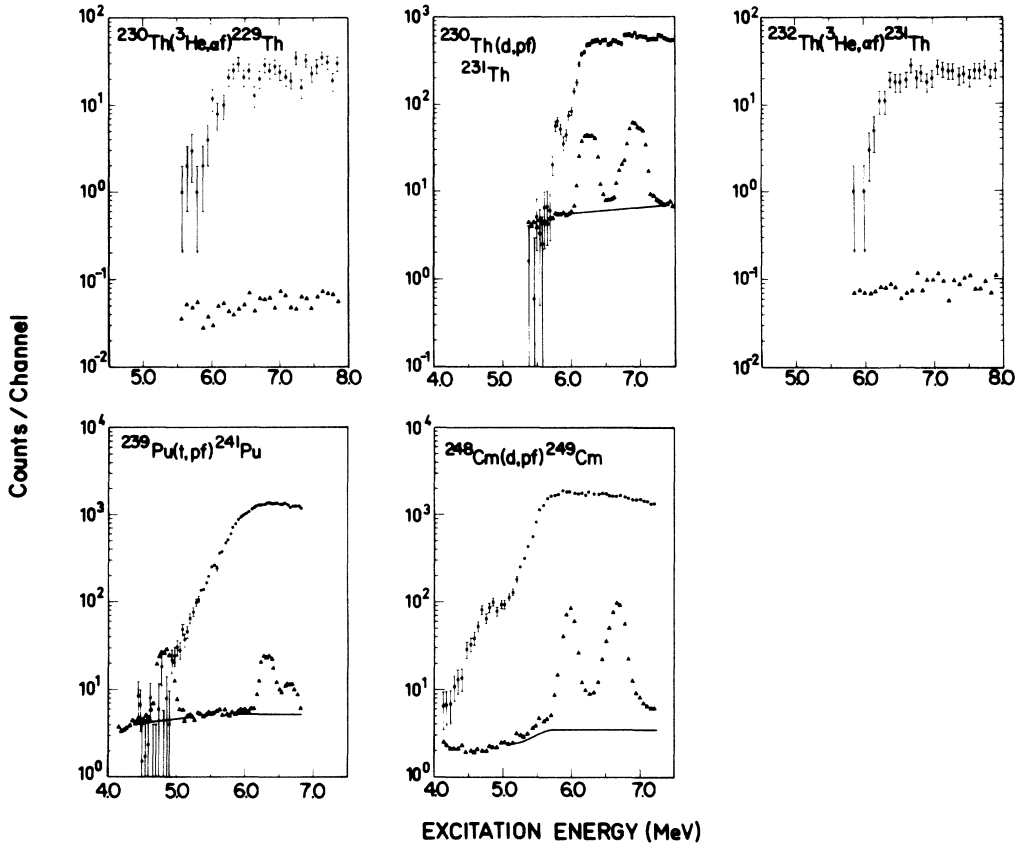

FIG. 2. Measured coincidence (circles) and singles spectra for a variety of reactions. Solid lines indicate interpolated singles cross sections for the target element. Singles spectra have been normalized to the level of the accidental contributions in the coincidence spectrum.

IV. STATISTICAL MODEL FOR ANALYSIS OF EXPERIMENTAL RESULTS

In the previous section it was seen that combining the results of the present experiments with previous (n,f), (d,pf), and (t,pf) data yields a comprehensive set of fission probability distributions for a wide range of actinide nuclei. By analyzing these results in a consistent manner it should then be possible to generate a set of experimental fission barrier parameters which can be used to look for general trends and to compare the theoretical calculations. In following sections we will discuss some of the general features of the statistical model which we have used to extract information on fission barrier properties from the experimental data. Also a discussion of the level densities used in the model and test calculations to illustrate the sensitivity of the calculated fission probability distributions to various assumptions are presented.

A more comprehensive discussion of the calculation of fission probabilities in a variety of limiting cases is given in Appendix II of Ref. 1 and in Ref. 11

A. Calculation of the fission probability

It is a central assumption in the statistical model used to analyze results from odd fissioning nuclei that the vibrational strength in the second well is completely mixed (or damped) into the other compound excitations. This implies that fission proceeds in two steps; first the nucleus moves from well I to well II and then from well II to fission. This picture is shown schematically in Fig. 8. In this limit the probability that a state of particular spin and parity at a particular excitation energy E will fission can be written as

$$P_f(EJ\pi) = \left\langle \frac{N_f(EJ\pi)}{N_f(EJ\pi)+N_n(EJ\pi)+N_\gamma(EJ\pi)} \right\rangle , \quad (1)$$

where $N_i(EJ\pi)$, the number of open decay channels, is equal to $2\pi\Gamma_i(EJ\pi)/D_I(EJ\pi)$, Γ_i is the decay width for each process, and $D_I(J\pi)$ is the average spacing of compound levels in the first well. The effective number of fission channels can be written as

$$N_f = \frac{N_A N_B}{N_A + N_B} f\left(\frac{W_{II}}{D_{II}}\right) , \quad (2)$$

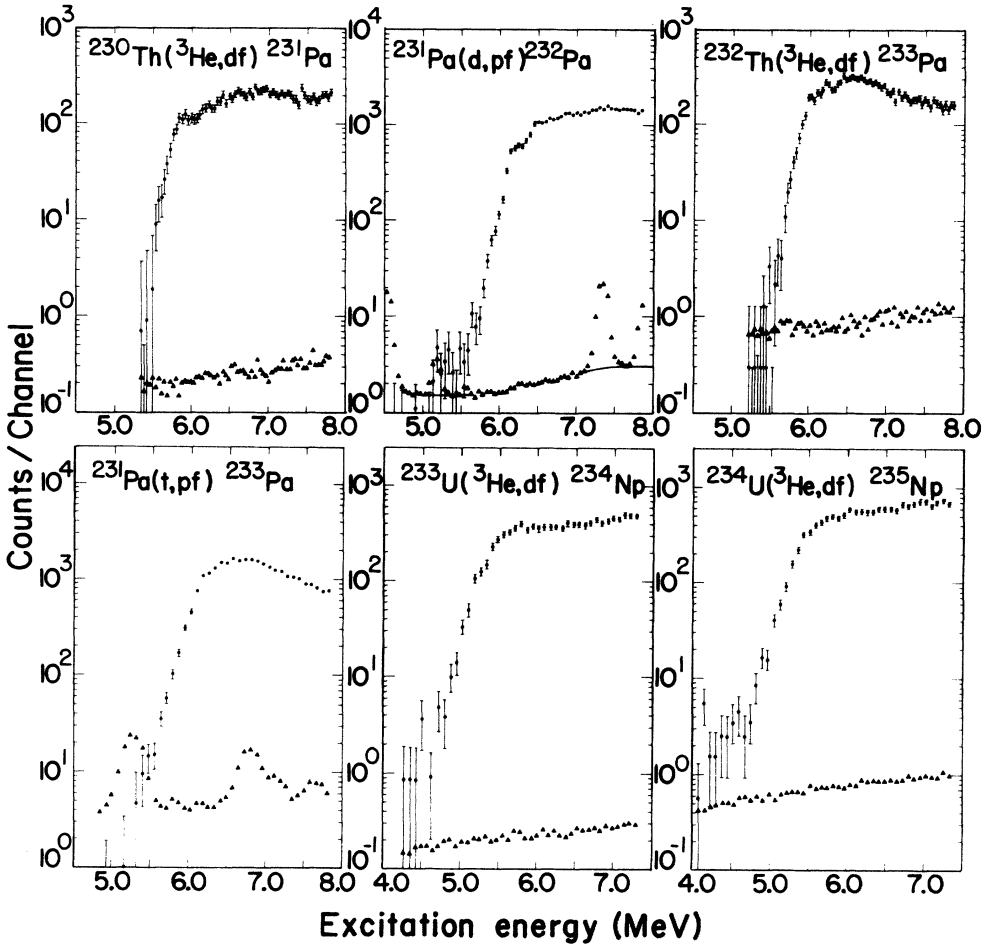

FIG. 3. Measured coincidence and singles spectra for a variety of reactions. See Fig. 2.

where N_A and N_B are the effective numbers of transition states at the two saddle points, W_{II} and D_{II} are the average width and spacing of levels in well II, and the function $f(W_{II}/D_{II})$ takes into account the coupling between levels in the first and second wells. If the levels in well II are very sharp then many of the more dense states in the first well will have only a small overlap with a state in the second well so that $f(W_{II}/D_{II})$ is small. Conversely, if the states in the second well are broader than their spacing then it is always possible to couple between the states in the two wells and $f(W_{II}/D_{II})$ approaches 1.

It has been shown in Refs. 1 and 11 that under the assumptions that the energy spread in the measurement is large compared to D_{II}, the line shape is Lorentzian, and the levels in well II are spaced equidistantly, the average fission probability can be written as

$$P_f(EJ\pi) = \frac{1}{[1 + a^2 + 2a \coth \frac{1}{2}(N_A + N_B)]^{1/2}}, \qquad (3)$$

where

$$a = \frac{(N_\gamma + N_n)(N_A + N_B)}{N_A N_B}.$$

Equation 3 is an approximation which neglects two effects: (1) the Porter-Thomas fluctuations in the over-all fission width and (2) the fluctuations in the spacings of individual levels in well II. The effect of Porter-Thomas fluctuations has been discussed in Refs. 1 and 3 and shown to be small when there is more than one open fission channel. The fluctuations in spacings in well II do not affect the fission probabilities in the limits $t \gg 1$ or $t \ll 1$ but could have a small effect in the region $t \sim 1$, where $t = N_A + N_B$. Neglect of these two fluctuation effects leads to a small overestimate of P_f calculated with the present model.

Finally, in the model the predicted fission probability is obtained by averaging over all possible angular momentum and parity values:

$$P_f(E) = \sum_{J\pi} \alpha(EJ\pi) P_f(EJ\pi),$$

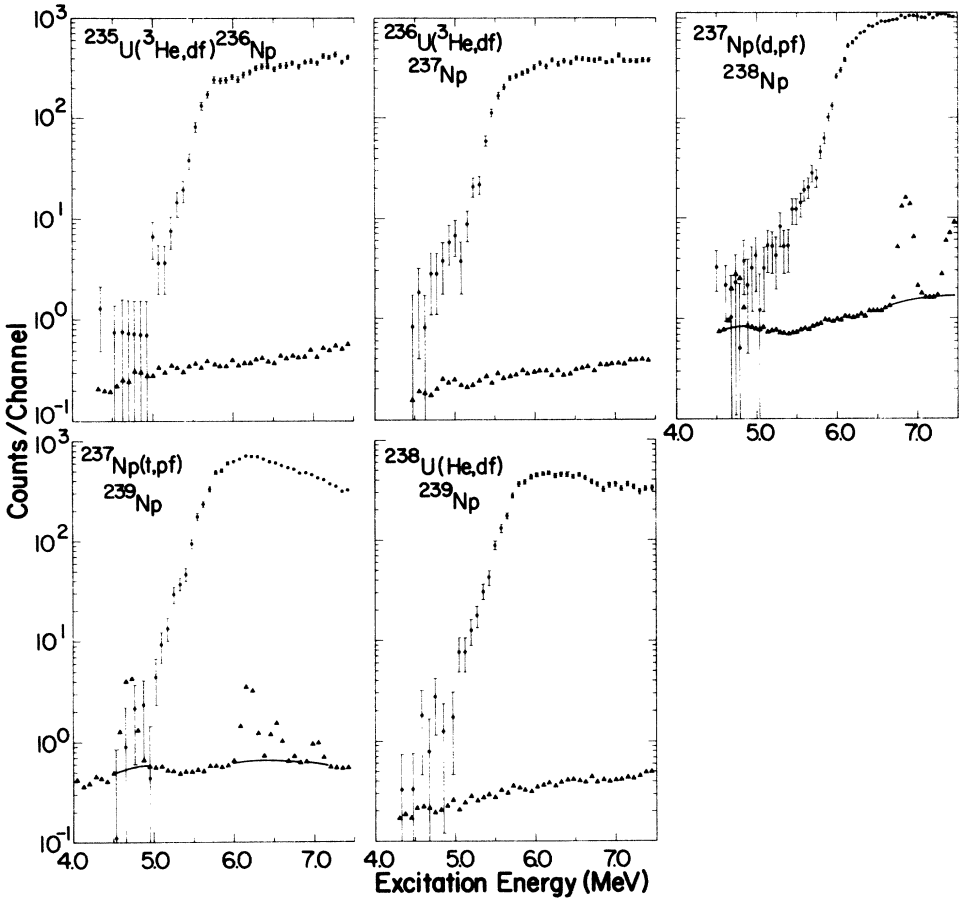

FIG. 4. Measured coincidence and singles spectra for a variety of reactions. See Fig. 2.

where $\alpha(EJ\pi)$ are the relative probabilities of exciting states with a particular $J\pi$ in the direct reaction. In the model the $\alpha(EJ\pi)$ coefficients are assumed to be energy independent and calculated as described in Ref. 1.

The calculation of the fission probability now reduces to a calculation of the number of decay channels N_A, N_B, N_n, and N_γ. For these quantities the expressions given in Ref. 12 are used, except that optical model transmission coefficients[13] were used in the N_n calculations. The N_γ values were normalized so that calculated values of Γ_γ reproduce measured values at the neutron binding energy for odd Pu isotopes.

As discussed in Sec. IV B, there are difficulties in some cases in estimating absolute values for the quantities N_n, N_γ, N_A, and N_B. To facilitate fitting of the experimental data two adjustable constants G_n and G_γ, which multiply the quantities N_n and N_γ, were introduced. As is seen in Eq. (1), the function P_f is not sensitive to the absolute values of the number of decay channels of a given type but is sensitive only to the ratios N_n/N_f and N_γ/N_f. Therefore, deviation of the values of G_n and G_γ from 1 can result from uncertainties in the N_f calculation as well as in the N_n and N_γ estimates. The experimental values obtained for the G_n and G_γ parameters and their significance are discussed in Sec. VI A.

B. Calculation of level densities

In a recent calculation of fission isomer excitation functions[12] a method was developed for obtaining level densities directly from the theoretical single particle level spectra at the appropriate deformations. However, this approach employed a saddle point approximation which is not adequate at excitation energies below 1 MeV in doubly even or odd-A nuclei where the specific character of the states involved in fission or neutron deexcitation becomes important. For this reason N_A, N_B, and N_n were calculated as a sum of two separate contributions when the decay involved an even-even nucleus (i.e., neutron decay from even Z, odd N) or an odd-A nucleus. The first contribution came

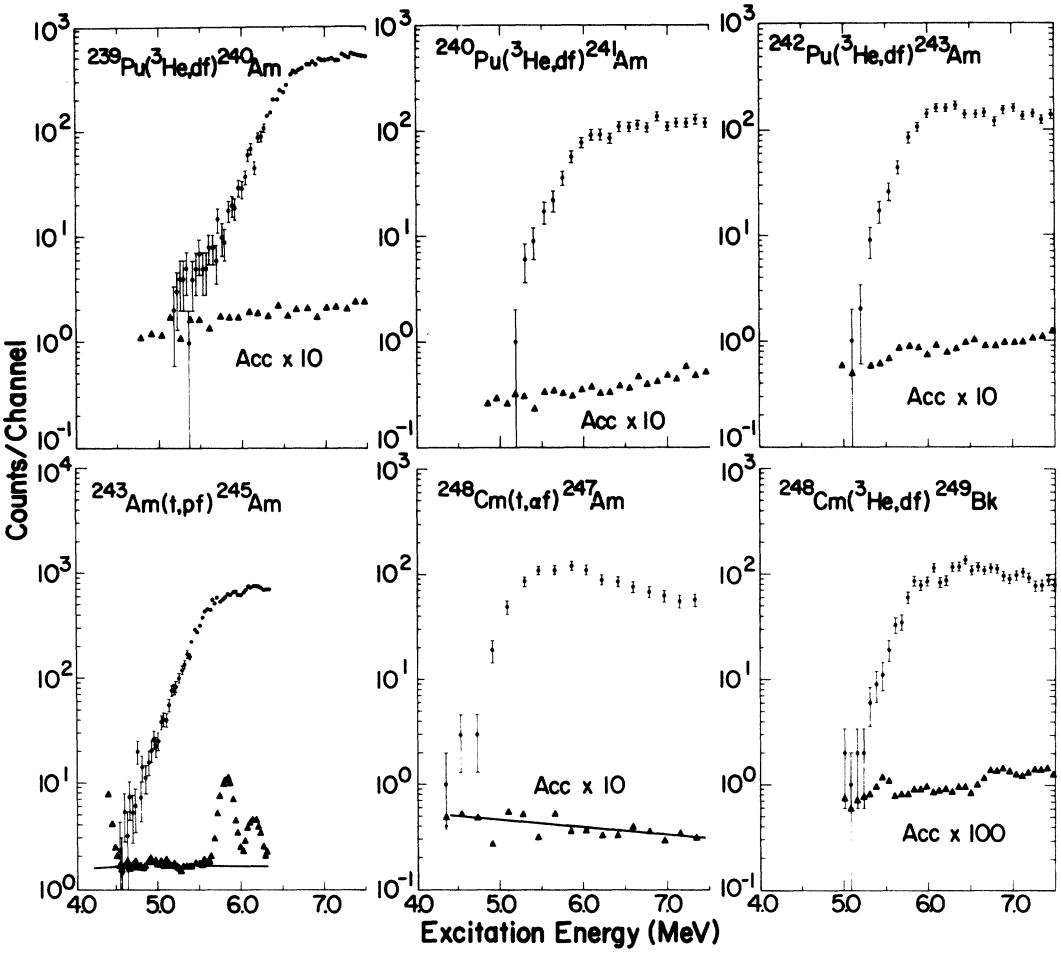

FIG. 5. Measured coincidence and singles spectra for a variety of reactions. See Fig. 2.

from states above 1 MeV where a continuous level density was used, whereas the second contribution from states below 1 MeV used a discrete spectrum of levels. The levels used are shown in Figs. 9–11 for the decay of even Z-odd N, odd Z-even N, and odd Z-odd N fissioning nuclei, respectively.

The continuous level densities were the same ones used in the fission isomer calculations.[12] They were determined from single particle spectra calculations for ^{240}Pu at the ground state deformation (including the hexadecapole deformation), at the first saddle (not including the stable γ deformation), and at the second asymmetric saddle. At the second saddle point the level densities are multiplied by 2 to take into account the two degenerate solutions at the mass asymmetric saddle point.[14] The enhancement[14] of the level densities due to the low-lying rotational levels has not been included but since P_f depends on ratios of level densities these factors should cancel to first order. One potentially serious effect that is

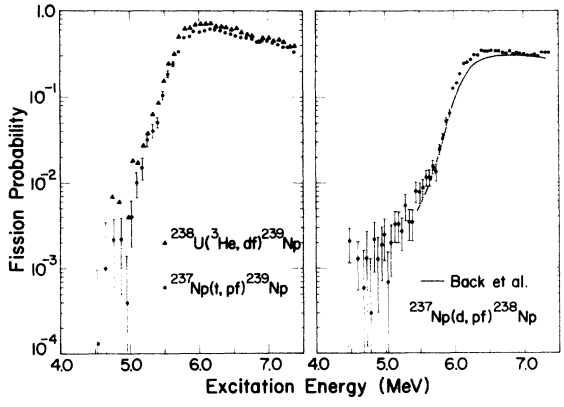

FIG. 6. Comparison of fission probability distributions for ^{239}Np excited by (t, p) and (^{3}He, d) reactions. Comparisons of results for the ^{237}Np(d, pf) reaction obtained in this experiment and reported previously by Back *et al.* (Ref. 3).

neglected is that caused by the additional rotational levels[14] that may be present at the first saddle point for those heavy nuclei which have axially asymmetric shapes at this saddle. In the present model the neglect of various level density enhancement effects should be compensated to first order by values of G_n and G_γ that are different from 1.

Level densities for odd nuclei were obtained by shifting the energy scale by Δ_n for odd N-even Z cases, by Δ_p for even N-odd Z cases, and by $\Delta_n+\Delta_p$ for odd N-odd Z cases where Δ_n and Δ_p are the pairing gaps at the ground state or appropriate saddle point deformations obtained in the microscopic single particle calculations. The continuous level densities were normalized to the measured density of $\frac{1}{2}^+$ states in ^{241}Pu at the neutron binding energy. The level densities for other spin states were calculated using a spin cutoff function with $\sigma = 5.5$. The level densities were assumed to be the same for both parities.

In principle the spectrum of discrete levels is different for each nucleus but in most cases it is not possible to obtain a very reliable estimate of the detailed discrete spectra, especially for those involved in the N_A and N_B calculations. Therefore, we have used a single discrete spectrum for the neutron and fission decay to each type of nucleus (even Z-odd N, odd Z-even N, or odd Z-odd N).

For neutron decay to an even-even residual nucleus we assume a spectrum of vibrational excitations (see Fig. 9) which are obtained from an average of the excitations experimentally observed in the uranium-curium region. Each vibration is assumed to contain a rotational band with spacings given by a rotational constant of 7 keV. For neutron decay to odd Z-even N nuclei (see Fig. 11) the discrete level spectrum is taken as

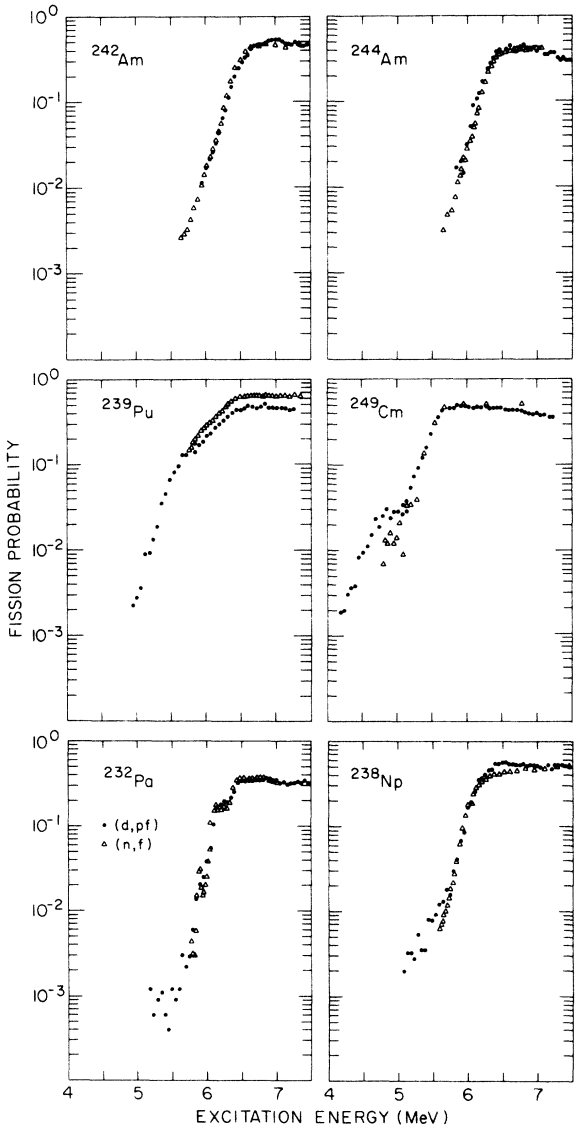

FIG. 7. Comparison of fission probability distributions obtained from (n, f) experiments with (d, pf) results for a variety of nuclei. The (d, pf) results have been corrected for contributions to the proton spectrum from deuteron breakup reactions as described in the text.

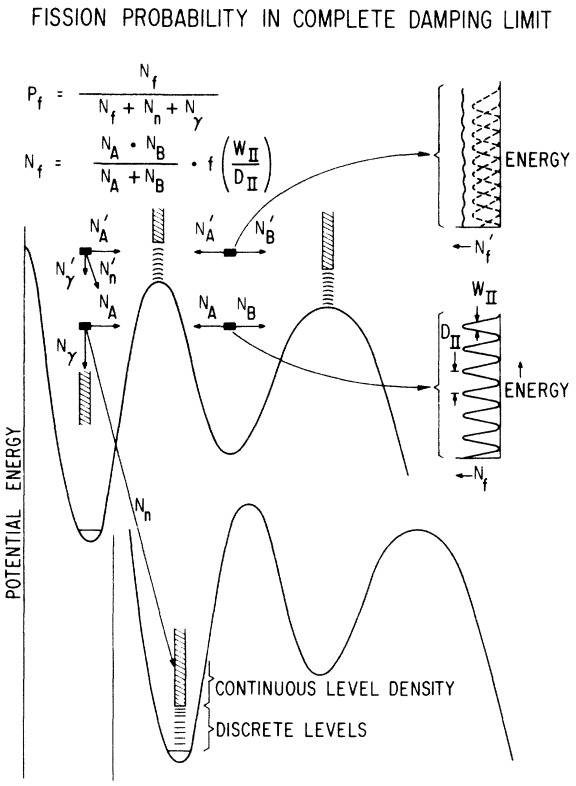

FIG. 8. A schematic illustration of the statistical model used to fit the experimental fission probability distributions.

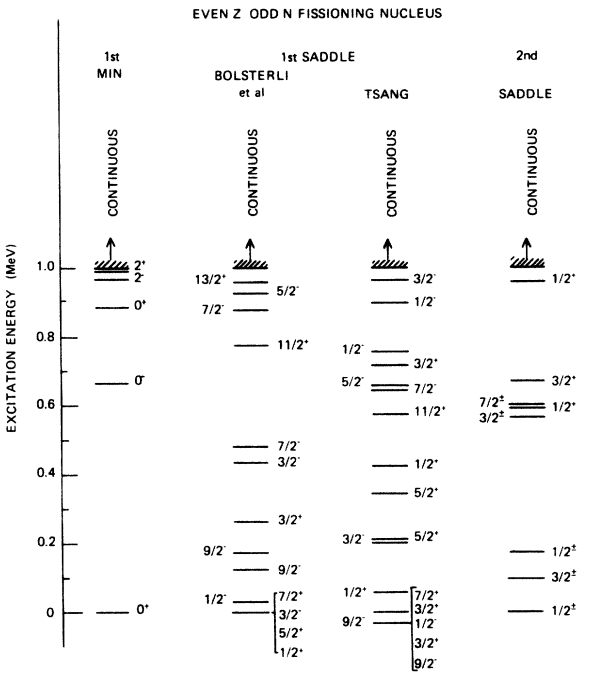

FIG. 9. Level spectra used in the calculations of N_n, N_A, and N_B for an even Z-odd N fissioning nucleus. Levels are obtained from the calculations of Bolsterli *et al.* (Ref. 15) and Tsang (Ref. 16) as described in the text.

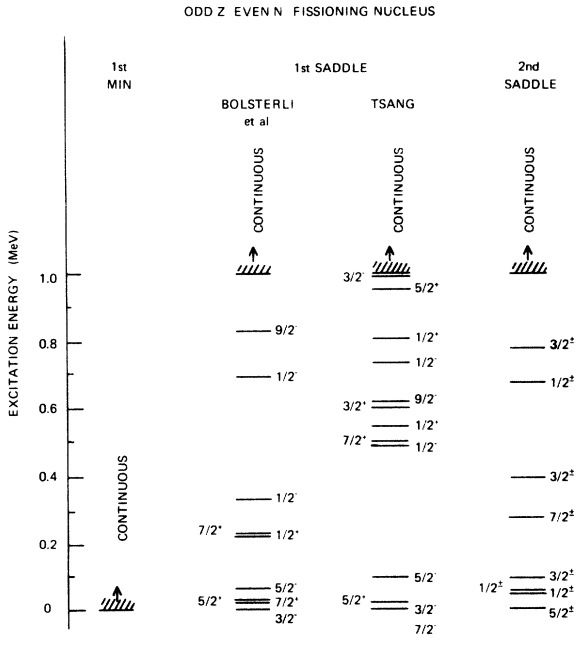

FIG. 10. Level spectra used in the calculations of N_n, N_A, and N_B for an odd Z-even N fissioning nucleus. Levels are obtained from the calculations of Bolsterli *et al.* (Ref. 15) and Tsang (Ref. 16) as described in the text.

the spectrum of one-quasiparticle proton states generated from the calculated[12,15] single proton states for ^{240}Pu. The energies of the one-quasiparticle states are obtained from the relation

$$E_q^i = (E_{sp}^{i\,2} + \Delta^2)^{1/2} - \Delta_0 ,$$

where Δ_0 and Δ are the pairing gaps at the ground states and at E_q^i, respectively. The pairing gap $\Delta(E)$ is obtained from the level density calculations[12] which use the same set of single proton states. Each one-quasiparticle state is assumed to have a rotational band built on it with a rotational constant of 7 keV.

For the fission decay of even Z-odd N nuclei (Fig. 9) and odd Z-even N nuclei (Fig. 10) the single neutron or single proton spectra[12,15] at the appropriate saddle points are used to generate one-quasiparticle states. These one-quasiparticle states are then used to calculate the contribution to N_A and N_B from the discrete levels for each case. At the second saddle the levels correspond to an asymmetric shape and are, therefore, taken as doubly degenerate. Such one-quasiparticle states are assumed to head a rotational band with a rotational constant of 5 keV.

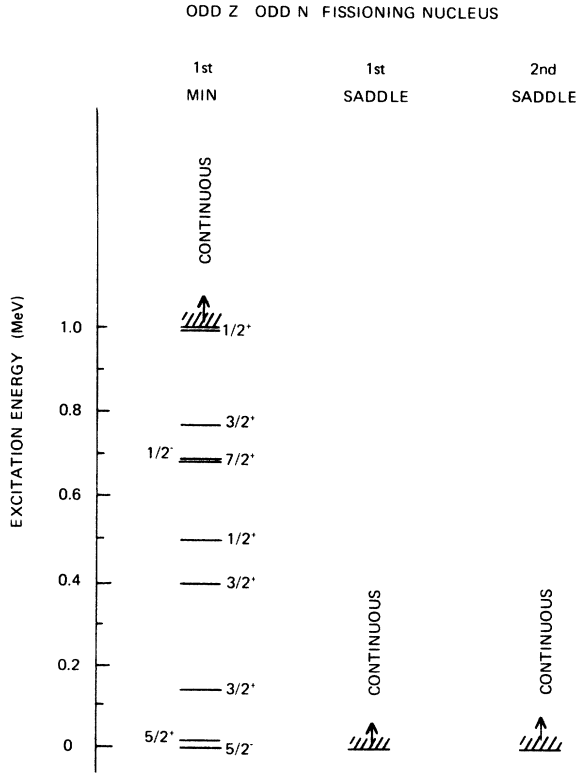

FIG. 11. Level spectra used in the calculations of N_n, N_A, and N_B for an odd Z-odd N fissioning nucleus. Levels are obtained from the calculations of Bolsterli *et al.* (Ref. 15) as described in the text.

Figures 9 and 10 also show discrete level spectra at the first saddle point taken from Tsang.[16] The details of the two sets of discrete spectra are different but the total number of levels available between 0 and 1 MeV are similar. This is illustrated better in Fig. 12 where the total discrete and continuous level densities are shown at the relevant deformations. Figure 12 also shows that below 1 MeV the continuous level density calculations considerably underestimate the level densities for doubly even and odd-A nuclei.

C. Sensitivity of the model to various effects

In order to test the sensitivity of our model calculations to the adopted level spectra, a series of test calculations were performed and the results are shown in Fig. 13. In sections (a) and (b) of the figure it is seen that the introduction of the discrete levels in the calculation of N_f produces a large shift in the apparent threshold whereas the calculations using levels predicted by Bolsterli *et al.*[15] or by Tsang[16] give very similar results. Thus, we conclude that the inclusion of the correct number of discrete levels is very important but the calculations are not very sensitive to the detailed ordering and spacing of the discrete levels. Sections (c) and (d) (Fig. 13) show that the inclusion of discrete levels in the neutron decay has a significant effect but not as great as the inclusion of the discrete fission levels.

Finally, in section (c) the effect of including the couplings between levels in the first and second wells is seen to be important only at energies below the top of the lowest peak of the barrier ($E_B = 5.50$ MeV in this case).

V. FITS TO EXPERIMENTAL RESULTS

The statistical model as described in Sec. IV contains a total of six adjustable parameters; E_A, $\hbar\omega_A$, E_B, $\hbar\omega_B$, G_n, and G_γ. In the analysis of the experimental fission probabilities it is usually possible to determine only three of these parameters and, therefore, estimates of some of the parameters must be taken from other sources. If one peak of the barrier is much higher than the other then the height and curvature of this peak is determined from the fit to the threshold energy and the slope of the fission probability. If both

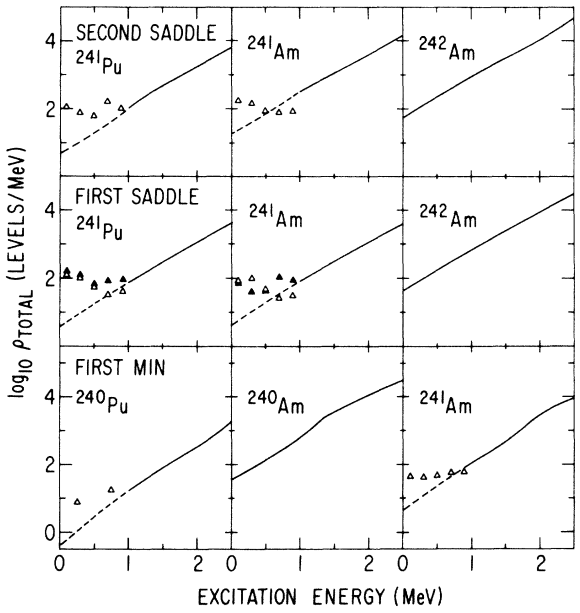

FIG. 12. Calculations of the total level density as a function of excitation energy. Solid and dashed lines show results obtained using the saddle point integration method. Open and closed triangles show estimates of the total density of discrete levels from the single particle spectra of Bolsterli *et al.* (Ref. 15) and Tsang (Ref. 16), respectively.

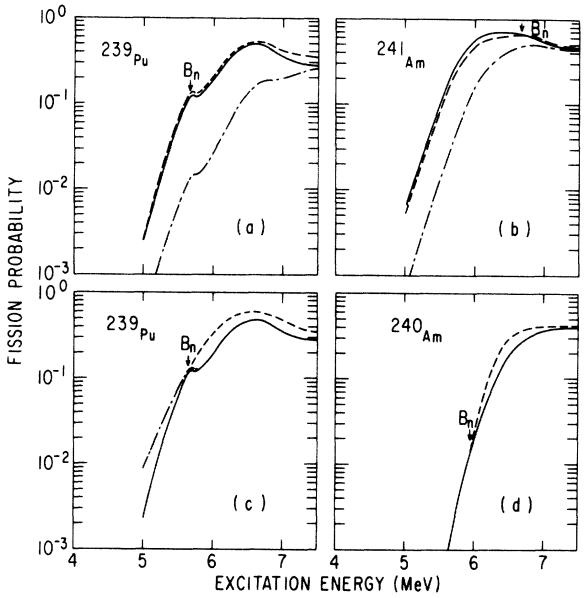

FIG. 13. Tests of the sensitivity of the theoretical calculations to various effects. The solid curves show calculations with the statistical model described in the text. The other curves use the same set of parameters with the following changes in the model: Sections (a) and (b), the dashed curve uses Tsang levels (Ref. 16) at the first saddle point and the dot-dashed curve shows the effect of replacing the discrete levels with the continuous level density at the first saddle point. Sections (c) and (d), the dashed curve shows the effect of replacing the discrete levels with the continuous level density at the first minimum. Section (c), the dot-dashed curve shows the effect of assuming strong coupling between levels in the first and second minima.

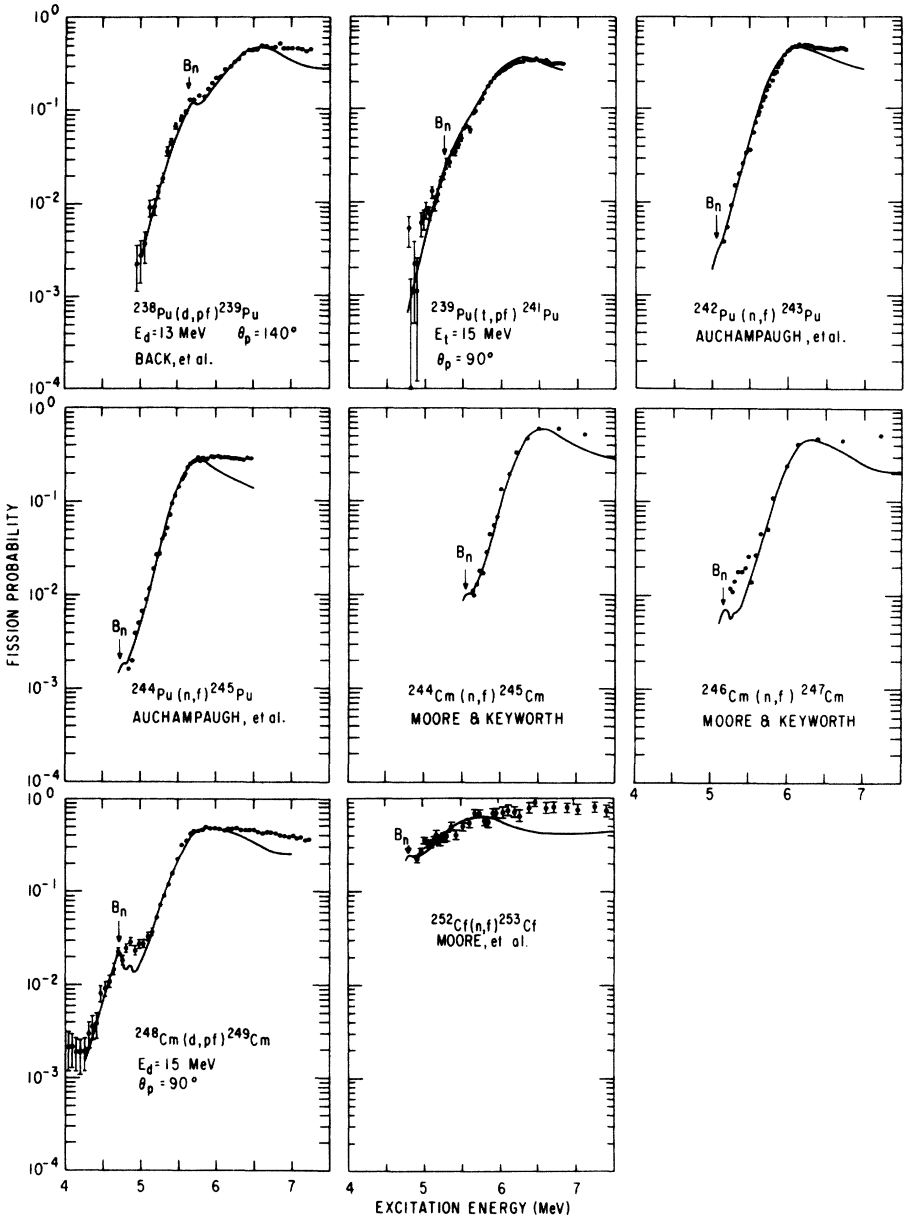

FIG. 14. Fission probability distributions for Pu, Cm, and Cf nuclei. Solid curves indicate theoretical fits with the statistical model described in the text. Data for (d, pf) and (n, f) reactions were taken from Refs. 3, 7–9.

peaks are of comparable heights then the height and curvature of one peak can be determined if the height and curvature of the other peak are known from some external source or, in some cases, estimates for both E_A and E_B can be obtained if $\hbar\omega_A$ and $\hbar\omega_B$ are fixed at reasonable values. The third parameter is either G_n or G_γ. For nuclei where the fission threshold is below B_n the maxima in the fission probabilities occur below the neutron binding energy and the fits are most sensitive to G_γ. For the few cases where B_n occurs near the fission threshold, estimates can be obtained for both G_γ and G_n (e.g., ^{239}Pu, ^{241}Pu, and ^{249}Cm). When the fission threshold is above B_n the fit is most sensitive to G_n.

A. Plutonium and heavier nuclei

In these nuclei E_A is greater than E_B and in many cases values for E_B and $\hbar\omega_B$ are known from the analysis of fission isomer data.[12] Thus, the calculated fission probability distributions are most sensitive to E_A and $\hbar\omega_A$ and estimates for E_B and $\hbar\omega_B$ can be obtained either from the

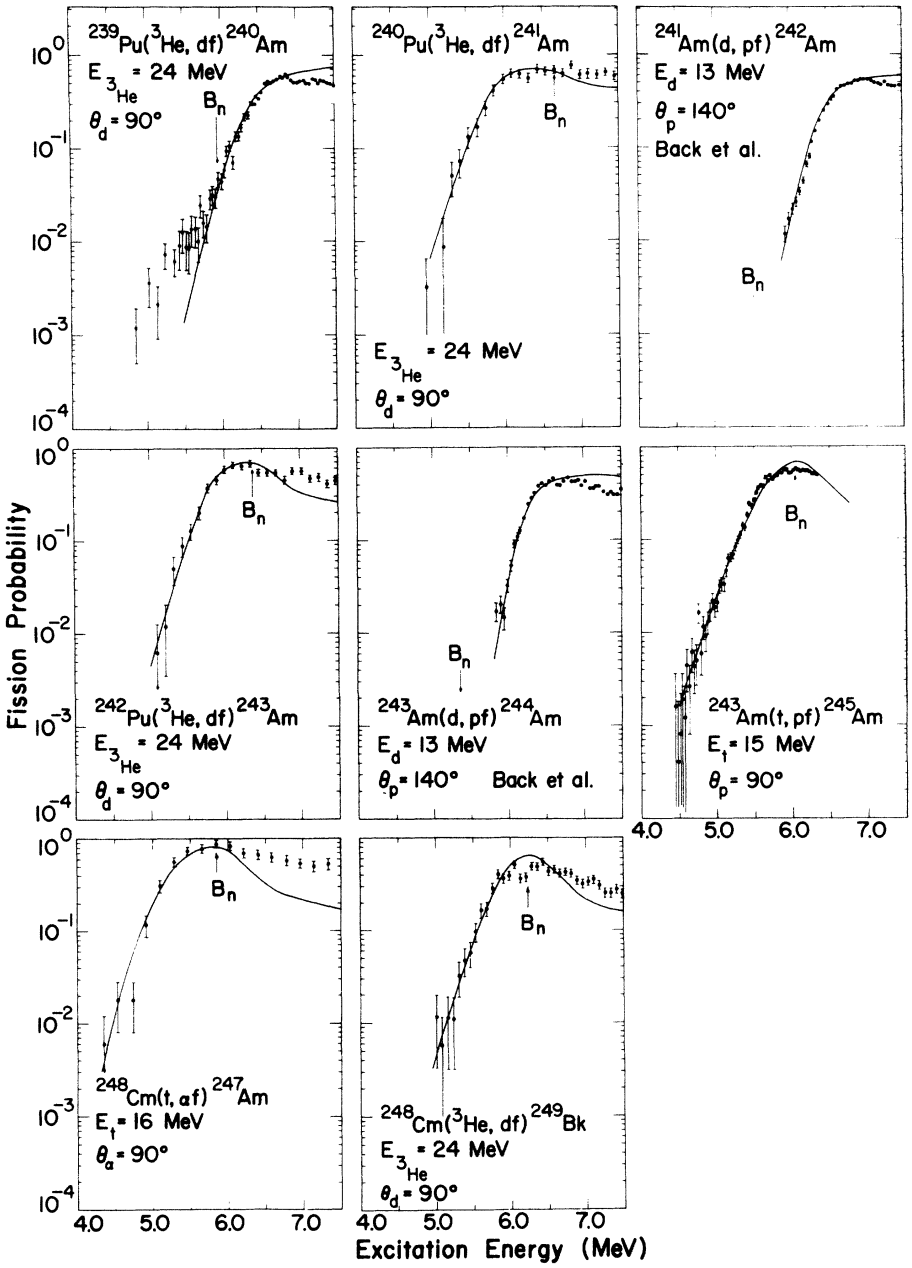

FIG. 15. Fission probability distributions for Am and Bk nuclei. Solid curves indicate theoretical fits with the statistical model described in the text. Data for (d, pf) reactions were taken from Ref. 3.

isomer results or from extrapolations of the isomer results from nearby nuclei. (For americium and heavier nuclei the difference in heights $E_A - E_B$ is generally greater than 1 MeV and the calculations are very insensitive to the values assumed for E_B and $\hbar\omega_B$.)

Theoretical and experimental fission probabilities in this mass region are shown in Figs. 14 and 15 and the parameters obtained from the fits are listed in Table II. In general the calculations reproduce the experimental fission probabilities in the threshold region but at high energies they tend to underestimate the fission probabilities for odd-A nuclei and predict too high fission probabilities for doubly odd nuclei. Possible causes of these systematic deviations will be discussed in Sec. VI. The errors quoted for E_A and $\hbar\omega_A$ include our estimates of the effects of systematic errors in the level densities used in the width calculations. The errors quoted for G_n and G_γ reflect only the experimental uncertainty in the absolute fission probability.

TABLE II. Barrier parameters estimated from analysis of experimental fission probability distributions. Values given in parentheses were estimated as described in the text and held fixed during fitting of the experimental data.

Nucleus	E_A	E_B	$\hbar\omega_A$	$\hbar\omega_B$	G_n	G_γ
^{229}Th	(6.02)	6.30 ± 0.20	(0.90)	0.65 ± 0.10	$0.70^{+0.46}_{-0.20}$	(1.0)
^{231}Th	(6.02)	6.22 ± 0.20	(0.90)	0.52 ± 0.10	$0.85^{+0.36}_{-0.20}$	(1.0)
^{233}Th	(6.02)	6.28 ± 0.20	(0.90)	0.45 ± 0.10	$0.90^{+0.38}_{-0.21}$	(1.0)
^{231}Pa	5.75 ± 0.30	5.85 ± 0.30	(0.8)	(0.45)	(0.3)	$3.5^{+2.1}_{-1.3}$
^{232}Pa	5.75 ± 0.30	6.10 ± 0.30	(0.6)	(0.45)	$0.45^{+0.20}_{-0.16}$	(3.5)
^{233}Pa	5.85 ± 0.30	6.00 ± 0.30	(0.8)	(0.40)	(0.3)	$1.8^{+1.5}_{-1.0}$
^{235}U	6.10 ± 0.30	5.65 ± 0.30	(0.85)	(0.50)	$0.30^{+0.22}_{-0.12}$	(2.5)
^{237}U	6.35 ± 0.30	5.95 ± 0.30	(0.85)	(0.55)	$0.12^{+0.07}_{-0.04}$	(2.5)
^{239}U	6.55 ± 0.30	6.30 ± 0.30	(0.90)	(0.65)	$0.05^{+0.03}_{-0.015}$	(2.5)
^{234}Np	5.35 ± 0.30	5.00 ± 0.30	(0.6)	(0.42)	(0.3)	$2.5^{+3.3}_{-2.2}$
^{235}Np	5.60 ± 0.30	5.20 ± 0.30	(0.8)	(0.55)	(0.3)	$3.5^{+3.0}_{-2.0}$
^{236}Np	5.70 ± 0.30	5.20 ± 0.30	(0.6)	(0.42)	(0.3)	$2.0^{+1.8}_{-1.2}$
^{237}Np	5.70 ± 0.30	5.50 ± 0.30	(0.8)	(0.55)	(0.3)	$2.8^{+2.4}_{-1.5}$
^{238}Np	6.00 ± 0.30	6.00 ± 0.30	(0.6)	(0.42)	$0.04^{+0.04}_{-0.02}$	(1.8)
^{239}Np	5.85 ± 0.30	5.50 ± 0.30	(0.8)	(0.55)	(0.3)	$1.8^{+2.0}_{-1.0}$
^{239}Pu	6.43 ± 0.20	(5.50)	1.00 ± 0.10	(0.55)	$0.30^{+0.26}_{-0.14}$	$0.75^{+0.12}_{-0.12}$
^{241}Pu	6.25 ± 0.20	(5.50)	1.10 ± 0.10	(0.55)	$0.30^{+0.20}_{-0.11}$	$1.15^{+0.40}_{-0.40}$
^{243}Pu	6.05 ± 0.20	(5.60)	0.80 ± 0.10	(0.55)	$0.15^{+0.13}_{-0.07}$	0.75
^{245}Pu	5.72 ± 0.20	(5.45)	0.90 ± 0.10	(0.55)	$0.40^{+0.27}_{-0.14}$	(1.2)
^{240}Am	6.35 ± 0.20	(4.80)	0.70 ± 0.10	(0.42)	$0.08^{+0.07}_{-0.04}$	(1.2)
^{241}Am	6.00 ± 0.20	(4.80)	0.80 ± 0.10	(0.55)	(0.3)	$1.8^{+1.5}_{-1.0}$
^{242}Am	6.38 ± 0.20	(4.80)	0.50 ± 0.10	(0.42)	$0.08^{+0.07}_{-0.04}$	(1.2)
^{243}Am	5.98 ± 0.20	(4.80)	0.75 ± 0.10	(0.55)	(0.3)	$1.8^{+1.3}_{-0.9}$
^{244}Am	6.18 ± 0.20	(4.80)	0.50 ± 0.10	(0.42)	$0.15^{+0.05}_{-0.04}$	(1.2)
^{245}Am	5.88 ± 0.20	(4.80)	0.85 ± 0.10	(0.55)	(0.3)	$1.8^{+1.7}_{-0.9}$
^{247}Am	5.60 ± 0.20	(4.80)	0.90 ± 0.10	(0.55)	(0.3)	(1.8)
^{245}Cm	6.38 ± 0.20	(4.20)	0.65 ± 0.10	(0.55)	$0.20^{+0.22}_{-0.12}$	(0.4)
^{247}Cm	6.20 ± 0.20	(4.20)	0.70 ± 0.10	(0.55)	$0.20^{+0.11}_{-0.08}$	(0.4)
^{249}Cm	5.80 ± 0.20	(4.20)	0.75 ± 0.10	(0.55)	$0.15^{+0.12}_{-0.07}$	$0.38^{+0.12}_{-0.12}$
^{249}Bk	6.05 ± 0.20	(4.20)	0.80 ± 0.10	(0.55)	(0.3)	$1.8^{+0.8}_{-0.6}$
^{253}Cf	5.60 ± 0.30	(4.20)	1.10 ± 0.10	(0.55)	0.15	2.5

B. Pa, U, and Np nuclei

The isotopes of Pa, U, and Np have $E_A \approx E_B$ and there is at present no independent information available on any of the barrier parameters. For these nuclei we first tried calculations with fixed values of $\hbar\omega_A$ and $\hbar\omega_B$ and allowed E_A and E_B to vary. From the systematics for nuclei in the Pu-Bk region we estimated $\hbar\omega_A = 0.8$ MeV and $\hbar\omega_B = 0.55$ MeV for odd-A nuclei, and $\hbar\omega_A = 0.6$

MeV and $\hbar\omega_B = 0.42$ MeV for doubly odd nuclei. With these values we obtained reasonable agreement with all of the experimental results for Np isotopes. For the U isotopes it was necessary to increase $\hbar\omega_A$ in order to correctly reproduce the shape of the fission probabilities, and for odd Pa isotopes $\hbar\omega_B$ had to be decreased slightly to obtain agreement with the experimental results. For all of these nuclei it is possible to reproduce the data with a range of correlated values for $\hbar\omega_A$ and $\hbar\omega_B$ so that the fits do not give a very significant determination of these quantities. Different combinations of $\hbar\omega_A$ and $\hbar\omega_B$ also lead to slightly different values for E_A and E_B for these nuclei.

The fits to the experimental data are shown in Figs. 16 and 17 and the corresponding parameters are listed in Table II. In most cases we again see that at high energies the calculations underestimate the fission probability for odd-A nuclei and overestimate it for odd-odd nuclei.

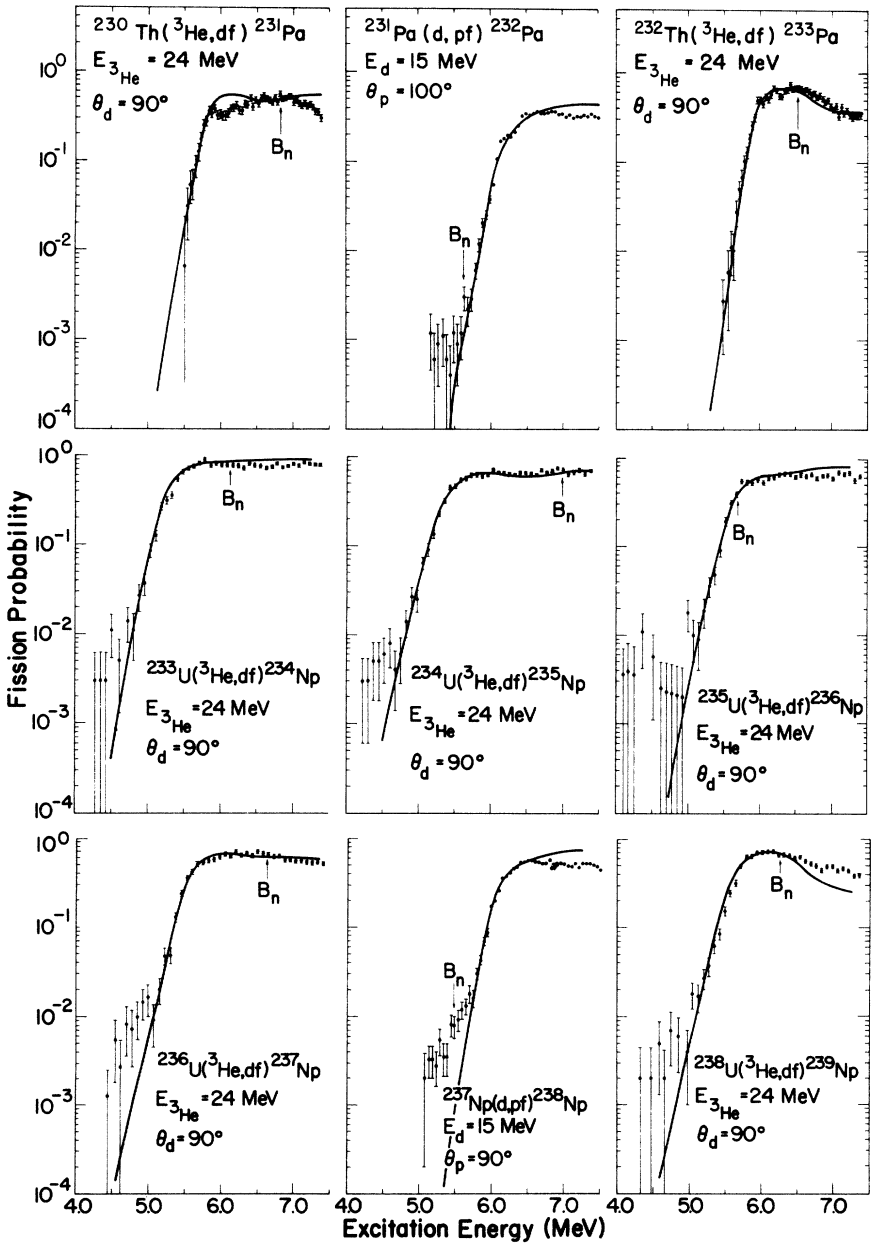

FIG. 16. Fission probability distributions for Pa and Np nuclei. Solid curves indicate theoretical fits with the statistical model described in the text.

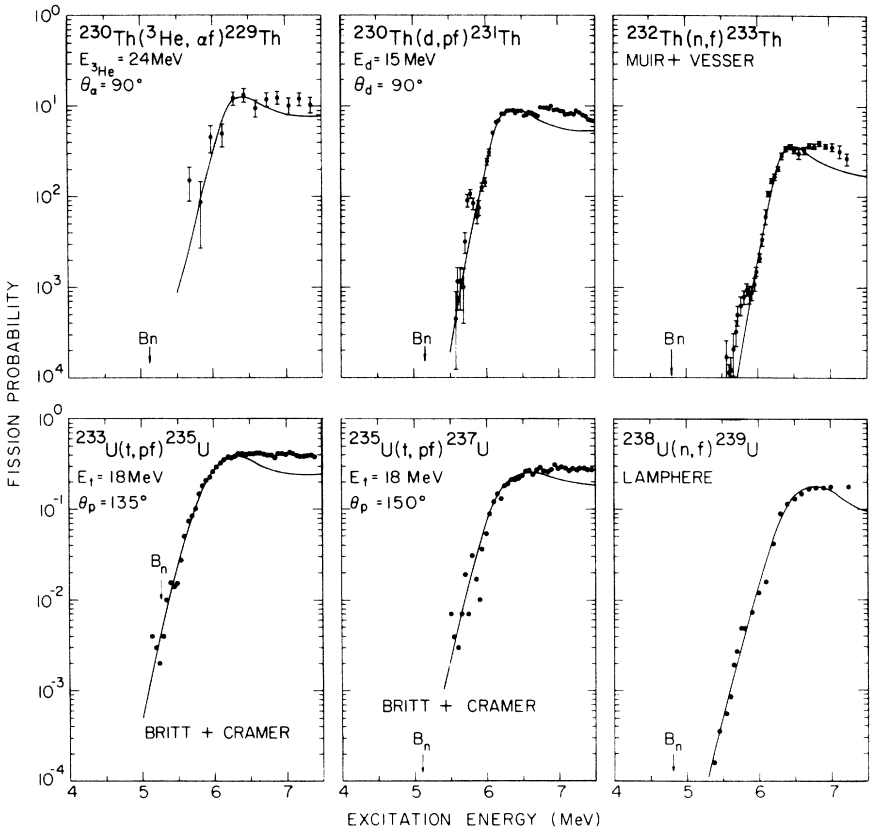

FIG. 17. Fission probability distributions for Th and U nuclei. Solid curves indicate theoretical fits with the statistical model described in the text. Data for (t, pf) and (n, f) reactions were taken from Refs. 4–6.

C. Thorium nuclei

For the thorium nuclei E_B is greater than E_A and a previous estimate of E_A and E_B has been obtained from an analysis[17] of the subbarrier fission resonance of ^{231}Th. In this case calculated fission probabilities are most sensitive to the second barrier, and consequently we used values of E_A and $\hbar\omega_A$ from the analysis by James, Lynn, and Earwaker,[17] of ^{231}Th for all three thorium isotopes and varied E_B and $\hbar\omega_B$ in the calculations. For ^{231}Th this type of analysis gave $E_B = 6.22$ MeV, $\hbar\omega_B = 0.52$ MeV in very good agreement with the values $E_B = 6.27$ MeV, $\hbar\omega_B = 0.57$ MeV obtained by James *et al.*[17] This agreement provides a consistency test for both analyses since James *et al.*[17] fitted the subbarrier resonance properties while we ignore the resonance and concentrate on reproducing the over-all behavior of the fission probability distribution.

The fits to the experimental data are shown in Fig. 17 and the corresponding parameters are listed in Table II.

VI. DISCUSSION

In general the estimates for barrier heights and curvatures (see Table II) are obtained from the energy and the slope of the measured fission probability near threshold while the normalization factors G_n and G_γ are sensitive to the absolute value of the fission probabilities. Therefore, errors in the absolute level densities used in the various width calculations are reflected primarily in the G_n and G_γ values. For example, if the ^{239}Pu and ^{241}Am data are refitted using the continuous level densities at all energies at the saddle points, the estimated values for E_A decrease by 0.3 and 0.2 MeV, respectively, and the values of G_n and G_γ change by factors of 3–6. This complete neglect of the discrete levels at the saddle point is an extreme limit and, thus, we conclude that uncertainties in the estimates of the discrete level spectra will not affect the barrier parameters within quoted errors but could lead to systematic errors in the G_γ and G_n values.

The reliability of the extracted barrier param-

eters can also be judged by comparison to barrier parameters obtained in other ways. As discussed in Sec. V C the E_B and $\hbar\omega_B$ values for ^{231}Th agree very well with values obtained by James *et al.*[17] from fits to the observed subbarrier resonance. In addition, comparisons to barriers extracted[3] for ^{238}Np, ^{239}Pu, ^{242}Am, and ^{244}Am using a very different statistical model show an average deviation from our values of ~0.06 MeV with maximum deviation of only 0.15 MeV.

A. Normalization factors G_n and G_γ

The values obtained for G_n and G_γ from the analysis of the experimental fission probability distributions are shown in Fig. 18. If the statistical model described in Sec. IV were adequate for describing these experimental results and the level spectra shown in Figs. 9–11 gave a good average representation of the level spectra involved in γ-ray, neutron, and fission decay, then we would expect $G_n = G_\gamma = 1$ within experimental uncertainties. The results in Fig. 18 show that in many cases the values of G_n and G_γ deviate significantly from unity. These deviations may arise from sources of two general types: (1) errors in defining the level spectra (Figs. 9–11) used in the various width calculations and (2) inadequacies in the statistical model which are compensated for by searching on the values of G_n or G_γ.

The major fundamental effect that has been neglected in our level spectra is the triaxial γ deformation at the first saddle point, an effect which has been predicted to be important for Pu and heavier nuclei.[18,19] Since the saddle point with a stable γ deformation corresponds to a shell region with a positive shell correction to the liquid drop surface and the axially symmetric saddle point corresponds to an "antishell" or negative shell correction, the single particle spectra at these two points might be significantly different. In particular, the increased shell energy would lead to a decrease in the density of the intrinsic states at low energies for the γ stable shape. However, the triaxial shape has a lower rotational symmetry and the total density of compound levels arising from each intrinsic state should be of the order of 5 times greater than for an axially symmetric shape.[14] Balancing these two factors probably still leads to a significantly larger density of compound states at a saddle point with a stable γ deformation.

At the second asymmetric saddle point the total energy surface is quite flat over a relatively large region so the exact position of the saddle point is difficult to locate and may change from nucleus to nucleus. This flat region corresponds to an approximate cancellation of strong variations in both the liquid drop and shell correction energies. Since the density of fission transition states is dependent primarily on the shell energy it may be difficult to define this spectrum even though the theoretical calculations may be adequate for calculating the total potential energy (liquid drop and shell energies) at the second saddle point. Further discussion of these points are given in Refs. 12 and 13. Also one must count the approximate treatment of the various fluctuation factors (see Ref. 1) as still another source of uncertainty in the derived G_n and G_γ factors.

In the following subsections we will briefly discuss some possible interpretations of the G_γ and G_n values in a few limiting cases but it should be kept in mind that there may be several factors contributing to the observed variations so that only the most general trends can be interpreted with a degree of significance.

1. Even Z-odd N nuclei; G_n

For even Z-odd N nuclei in the first 1 MeV of excitation energy above the neutron binding energy, Γ_n is calculated using average experimental levels in the residual even-even nucleus (see Fig. 9) and should be reasonably reliable. In this case deviations of G_n from 1 presumably reflect errors in the assumptions on the transition state level density at one or both saddle points. The results in Fig. 18 show that for these cases G_n decreased from a value of ~1 for Th nuclei to a value of ~0.2 for Cm nuclei. The average value $G_n \sim 0.2$ for Cm nuclei may indicate that the neglect of axially asymmetric deformations leads to an underestimation of the density of transition states of approximately a factor of 5. In contrast, for the Th nuclei, fission is dominated by the second barrier which presumably corresponds to the case $G_n \approx 1$.

For neutron decay energies above 1.0 MeV we have used a continuous level density and the results shown in Figs. 14 and 17 indicate that the calculated fission probabilities systematically decrease too rapidly in this region. This result may indicate that the continuous level densities are too large at least at the lowest energies. Consistent with this conclusion are the low values of G_n for cases where the fission threshold occurs more than 1 MeV above the neutron threshold (see ^{237}U and ^{239}U).

2. Odd-Z nuclei; G_n

For odd-Z nuclei at energies above the peak in the fission probability distribution the calculations systematically overestimate P_f for odd-odd nuclei

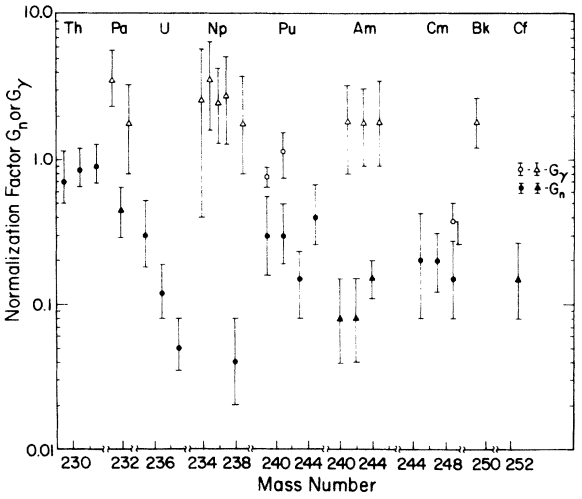

FIG. 18. Normalization factors G_n and G_γ obtained from fits to the fission probability distributions.

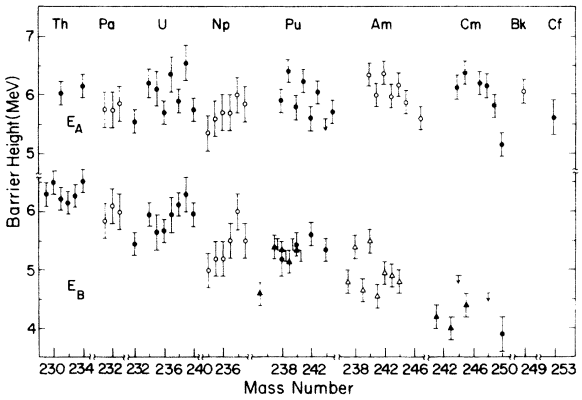

FIG. 19. Fission barrier heights obtained from fits to the fission probability distributions. Results for even-even nuclei are taken from Ref. 1. Triangles indicate estimates of E_B taken from Ref. 12.

and underestimate P_f for odd-even nuclei (see Figs. 15 and 16). These cases involve odd-odd nuclei in the Γ_f and Γ_n calculations, respectively, and the deviations suggest that we are systematically overestimating the slope of the level densities for odd-odd nuclei at the lowest energies. This result is similar to the conclusion for even-even nuclei at energies above 1 MeV (see Sec. VI A 1).

The values for G_n obtained from odd-odd nuclei are generally about 2 times lower than would be expected from the systematics of nearby even-Z nuclei. This suggests a systematic discrepancy for the estimated levels for odd-Z relative to even-Z nuclei but it is not possible to determine whether this discrepancy occurs in the neutron levels, the fission levels, or both.

3. G_γ

If the deviations of G_n from 1 are primarily due to underestimates of the density of transition states then we might expect $G_\gamma \approx G_n$, but the results shown in Fig. 18 indicate that this is not the case. For the three cases (^{239}Pu, ^{241}Pu, and ^{249}Cm) where G_γ and G_n can both be determined in the same nucleus we find that $G_\gamma \approx 3G_n$. Most of the other determinations of G_γ are very uncertain but they generally lie in the range of 2–10 times the values for G_n in neighboring nuclei. The reasons for this systematic difference between G_n and G_γ are not understood.

B. Systematics of the barrier heights

The barrier heights determined from the analysis of the experimental fission probabilities are listed in Table II and plotted in Fig. 19. Also plotted in Fig. 19 are results for E_B obtained[12] from the analysis of fission isomer excitation functions and E_A, and E_B values for even-even nuclei discussed in a previous paper.[1] In the previous paper the E_A and E_B values for even-even nuclei were compared with various theoretical calculations and this comparison will not be repeated here.

The most remarkable feature of these experimental barriers is the relative constancy of E_A at $\sim 6 \pm 0.5$ MeV over the entire region from Th through Cf and the steady decrease of E_B from ~ 6.3 MeV in Th to ~ 4 MeV for Cm isotopes.

Superimposed on these trends are some apparent odd-even fluctuations in E_A (and possibly in E_B for Am isotopes—see Ref. 12 for more discussion). For U, Pu, and Am isotopes the results show E_A values that are 0.3–0.5 MeV greater for odd-N than for even-N isotopes but this effect is not apparent in the Pa and Np isotopes. For the Cm isotopes the odd-even fluctuations could be masked by the anomaly[20] in the E_A values as the $N = 152$ shell is crossed. For the Am isotopes an odd-even fluctuation of the same magnitude also occurs in the ground state masses[21] and so our results indicate no odd-even fluctuation in the saddle point masses when measured relative to a spherical liquid drop mass surface. For the U and Pu nuclei the odd-even fluctuation in the saddle point masses determined in the same way would be even greater than those observed in the E_A values. The apparent odd-even fluctuations should be viewed with some caution, however, because the even-N nuclei involve competition between fission and γ emission near threshold whereas the odd-N nuclei have fission thresholds above the neutron binding energy. Therefore, systematic errors in the estimates of Γ_γ relative to Γ_n could lead to spurious odd-even

effects. At present we believe that the ±0.2 MeV uncertainties in E_A for these nuclei are realistic but as noted in the previous section the normalizations of the various decay widths are not completely understood.

We are grateful to A. Friedman and J. Lerner at Argonne National Laboratory for preparing the ^{248}Cm target. It is a pleasure to acknowledge useful discussions with S. Bjørnholm, A. Bohr, J. R. Huizenga, J. E. Lynn, B. Mottelson, J. R. Nix, and R. Vandenbosch. We would like to thank B. H. Erkkila for his help in initially setting up these experiments. We would also like to thank the Neutron Cross Section Group at Brookhaven National Laboratory for providing tabulations of current (n,f) cross section data for many isotopes of interest. One of us (BBB) acknowledges support from Staten naturvidenskabelige forskningsrad, Denmark. One of us (HCB) acknowledges the hospitality of the Nuclear Structure Research Laboratory, University of Rochester, where part of this manuscript was prepared, and support from the Japan Exhibition Commemorative Association for travel to the Niels Bohr Institute in Copenhagen during the preparation of this manuscript. One of us (BL) acknowledges fellowship support from NATO during his stay in Los Alamos.

---

*Work supported by the U.S. Atomic Energy Commission.

†Permanent address: Niels Bohr Institute, University of Copenhagen, Copenhagen, Denmark.

‡Permanent address: University of Bordeaux, Bordeaux, France.

§Permanent address: Brookhaven National Laboratory, Upton, New York 11973.

[1]B. B. Back, O. Hansen, H. C. Britt, and J. D. Garrett, Phys. Rev. C 9, 1924 (1974).

[2]J. P. Bondorf, Phys. Lett. 31B, 1 (1970).

[3]B. B. Back, J. P. Bondorf, G. A. Otroschenko, J. Pedersen, and B. Rasmussen, Nucl. Phys. A165, 449 (1971).

[4]D. W. Muir and L. R. Veeser, in Proceedings of the Third Conference on Neutron Cross Sections and Technology, Knoxville, Tennessee, 1971, CONF-710301, Vol. 1, p. 292; see also Los Alamos Scientific Laboratory Report No. LA-4648-MS (unpublished).

[5]R. W. Lamphere, Nucl. Phys. 38, 561 (1962); Phys. Rev. 104, 1654 (1956).

[6]H. C. Britt and J. D. Cramer, Phys. Rev. C 2, 1758 (1970).

[7]G. F. Auchampaugh, J. A. Farrell, and D. W. Bergen, Nucl. Phys. A171, 31 (1971).

[8]M. S. Moore and G. A. Keyworth, Phys. Rev. C 3, 1656 (1971).

[9]M. S. Moore, J. H. McNally, and R. D. Baybarz, Phys. Rev. C 4, 273 (1971).

[10]The (n, f) cross section data was provided by the Brookhaven National Laboratory Neutron Cross Section Group and came from the following original sources: ^{232}Pa—D. W. Muir and L. R. Veeser, Los Alamos Scientific Laboratory Report No. LA-4648-MS; ^{238}Np—W. K. Brown, D. R. Dixon, and D. M. Drake, Nucl. Phys. A156, 609 (1970); ^{239}Pu—M. G. Silbert, Los Alamos Scientific Laboratory Report No. LA-4108-MS; ^{249}Cm—M. S. Moore and G. A. Keyworth, Phys. Rev. C 3, 1656 (1971); ^{242}Am—P. A. Seeger, Los Alamos Scientific Laboratory Report No. LA-4420; ^{244}Am—D. K. Butler and R. K. Sjoblom, Phys. Rev. 124, 1129 (1961).

[11]J. E. Lynn and B. B. Back, J. Phys. A 7, 395 (1974).

[12]H. C. Britt, M. Bolsterli, J. R. Nix, and J. L. Norton, Phys. Rev. C 7, 801 (1973); H. C. Britt, S. C. Burnett, B. H. Erkkila, J. E. Lynn, and W. E. Stein, *ibid.* 1444 (1971).

[13]These transmission coefficients were obtained using the code ABACUS and optical model parameters from L. Rosen, J. G. Beery, A. S. Goldhaber, and E. H. Auerbach, Ann. Phys. (N.Y.) 34, 96 (1965).

[14]S. Bjørnholm, A. Bohr, and B. R. Mottelson, in Proceedings of the Third International Atomic Energy Symposium on Physics and Chemistry of Fission, Rochester, 1973 (to be published).

[15]M. Bolsterli, E. O. Fiset, J. R. Nix, and J. L. Norton, Phys. Rev. C 5, 1050 (1972).

[16]C. F. Tsang, private communication; S. G. Nilsson, C. F. Tsang, A. Sobiczewski, A. Szymanki, S. Wycech, C. Gustafsson, I. L. Lamm, P. Moller, and B. Nilsson, Nucl. Phys. A131, 1 (1969).

[17]G. D. James, J. E. Lynn, and L. G. Earwaker, Nucl. Phys. A189, 225 (1972).

[18]S. E. Larsson, I. Ragnarsson, and S. G. Nilsson, Phys. Lett. 38B, 269 (1972).

[19]V. Gotz, H. C. Pauli, and K. Junker, Phys. Lett. 39B, 436 (1972).

[20]B. B. Back, O. Hansen, H. C. Britt, and J. D. Garrett, Phys. Lett. 46B, 183 (1973).

[21]W. D. Myers and W. J. Swiatecki, Ark. Fys. 36, 343 (1967).